

1 **Optogenetic activation of muscle contraction *in vivo***

2 Elahe Ganji^{1,2,3}, C. Savio Chan⁴, Christopher W. Ward⁵, Megan L. Killian^{2,3}

3 1. Department of Mechanical Engineering, University of Delaware, Newark, Delaware,

4 2. Department of Biomedical Engineering, University of Delaware, Newark, Delaware,

5 3. Department of Orthopaedic Surgery, Michigan Medicine, Ann Arbor, Michigan, 48109

6 4. Department of Physiology, Feinberg School of Medicine, Northwestern University, Chicago,

7 IL, USA

8 5. Department of Orthopaedics, University of Maryland School of Medicine, Baltimore, MD

9 21201, USA

10 **Corresponding Author**

11 Megan L. Killian, PhD

12 University of Michigan Medical School

13 Department of Orthopaedic Surgery

14 2021 BSRB, 109 Zina Pitcher Place, Ann Arbor, Michigan 48109

15 Phone: 734-615-5388, E-mail: mlkillia@med.umich.edu

16 **Author contributions**

17 EG and MLK conceived of the study; EG drafted the manuscript; EG and MLK designed the

18 experiments; EG and CG developed experimental methodologies; CSC and MLK developed

19 mouse models; CWW assisted with *in vivo* experimental setup; EG executed experiments; EG,
20 CSC, CWW, and MLK wrote, edited, and approved the final manuscript.

21 Acknowledgements: Thanks to Dr. Gwen Talham and Frank Warren for assistance with animal
22 care; Matthew Hudson and Brittany Wilson for sharing use of the Aurora 3-in-1 *in vivo* system;
23 Jaclyn Soulas for assistance with whole mount imaging of the triceps surae; and Harrah Newman
24 for preliminary power meter studies.

25 Funding: Eunice Kennedy Shriver National Institute of Child Health and Human Development
26 (R03 HD094594 to MLK) and The National Institute of Neurological Disorders and Stroke (R01
27 NS069777 to CSC).

28

29 **Abstract**

30 Optogenetics is an emerging alternative to traditional electrical stimulation to initiate
31 action potentials in activatable cells both ex vivo and in vivo. Optogenetics has been commonly
32 used in mammalian neurons and more recently, it has been adapted for activation of
33 cardiomyocytes and skeletal muscle. Therefore, the aim of this study was to evaluate the
34 stimulation feasibility and sustain isometric muscle contraction and limit decay for an extended
35 period of time (1s), using non-invasive transdermal light activation of skeletal muscle (triceps
36 surae) in vivo. We used inducible Cre recombination to target expression of Channelrhodopsin-2
37 (ChR2(H134R)-EYFP) in skeletal muscle (Acta1-Cre) in mice. Fluorescent imaging confirmed
38 that ChR2 expression is localized in skeletal muscle and does not have specific expression in
39 sciatic nerve branch, therefore, allowing for non-nerve mediated optical stimulation of skeletal
40 muscle. We induced muscle contraction using transdermal exposure to blue light and selected
41 10Hz stimulation after controlled optimization experiments to sustain prolonged muscle
42 contraction. Increasing the stimulation frequency from 10Hz to 40Hz increased the muscle
43 contraction decay during prolonged 1s stimulation, highlighting frequency dependency and
44 importance of membrane repolarization for effective light activation. Finally, we showed that
45 optimized pulsed optogenetic stimulation of 10 Hz resulted in comparable ankle torque and
46 contractile functionality to that of electrical stimulation. Our results demonstrate the feasibility
47 and repeatability of non-invasive optogenetic stimulation of muscle in vivo and highlight
48 optogenetic stimulation as a powerful tool for non-invasive in vivo direct activation of skeletal
49 muscle.

50

51 **Introduction**

52 Contactless optical control of action potentials (APs) using optogenetics is an emerging
53 alternative to traditional electrical stimulation for initiating contractions in skeletal and smooth
54 muscles. Optogenetics utilizes light responsive microbial photosensitive proteins (opsins) to
55 translocate ions across lipid membranes, enabling precise (targeted cell-specific) and fast
56 (millisecond [ms]-time scales) optical control of membrane voltages.^{1,2} Channelrhodopsin-2
57 (ChR2) is a commonly used seven-layer transmembrane example of the light-sensitive opsins
58 that acts as a non-specific inward cation channel (depolarizing) with an intrinsic light
59 sensitivity.^{3,4} Targeted expression of ChR2 has been commonly used as a tool for the repeatable
60 and high-kinetic targeted activation of, most commonly, mammalian neurons^{1,2,5} and, more
61 recently, cardiomyocytes⁶ with light. In heart, ChR2 expression in cardiomyocytes has been
62 mediated by non-viral delivery of exogenous light-sensitive ChR2 (e.g., tandem cell units)⁷; viral
63 ChR2 expression with CAG promoters in embryonic stem cells⁸; and transgenic mouse lines
64 expressing ChR2.⁸ Enabled by these approaches, optical activation has been shown a promising
65 strategy to address cardiac arrhythmia and explore cardiac development.^{8,9} Optogenetics
66 applications, Typically, muscle activation is initiated by the motor neuron whose voltage-
67 dependent release of acetylcholine into the neuromuscular junction (NMJ) initiates the sodium
68 (Na⁺) channel activation and local post-synaptic cation influx (Na⁺) and efflux (K⁺) the muscle
69 cell transmembrane whose threshold depolarization initiates action potentials (APs) in the
70 muscle fiber, however, are not limited to neurons and cardiac muscle cells.

71 Optogenetics is a promising tool in skeletal muscle activation both ex vivo and in vivo.
72 Skeletal muscle activation can be achieved approaches either using a neuron-mediated excitation
73 through presynaptic ion channels (indirect; electrical and optogenetic stimulation) or

74 transmembrane-mediate excitation through post-synaptic channels (direct; optogenetic
75 stimulation). Ex vivo, synchronous contraction at high (tetanus-like, sustained contraction) and
76 low frequency (twitch-like contraction) has been induced by photoactivation of ChR2 expressing
77 multinucleated myotubes (C2C12).¹⁰ Contactless optogenetic control of myotube contraction,
78 with high temporal resolution, circumvents technical challenges faced in ex vivo electrical
79 stimulation (e.g. electrode electrolysis and tissue damage).¹⁰ *In vitro*, contraction in explanted
80 soleus muscle is induced with photoactivation of mouse skeletal muscle with targeted expression
81 of ChR2 in enabled of muscles *in vitro*.¹¹ *In vivo*, light-stimulated control of mice with non-
82 specific expression of ChR2 in skeletal muscle sarcolemma and T-tubule (Sim1-Cre) has been
83 studied for restoration of function in denervated muscles.¹² Electrical stimulation, although with
84 high temporal resolution in neural stimulation, lacks the spatial specificity of optogenetic
85 stimulation in targeting cell subpopulations based on morphological markers and molecular
86 footprint even in single cell intracellular electrical-stimulation approaches, are limited to in vitro
87 scenarios and cannot be used simultaneous in vitro stimulation of multiple single neurons or *in*
88 *vivo*.^{13,14} Optogenetics, on the contrary has excellent spatiotemporal resolution and is cell-
89 specific light-responsiveness to change transmembrane voltage.^{1,2} This spatiotemporal specificity
90 of optogenetics, prompts its potential to be utilized in conjunction with denervation models,
91 using either indirect approaches that target secondary motor cortex or sub-population of neurons
92 in the peripheral nervous system¹⁵ or using direct activation of muscle cell, sarcolemma, or T-
93 tubules.¹² Finally, optogenetic activation of skeletal muscle has potential in mitigating some of
94 these existing limitations in electrical stimulation approaches (i.e. tissue-damage caused by
95 repeated needle electrode placement, especially in juvenile animals, and limited applicability in
96 conjunction with denervation models).

97 Herein we report our development and validation of an optogenetic method for the direct
98 (non-nerve mediated) activation of skeletal muscle *in vivo*. The goal of this study was to develop
99 a method for sustaining muscle contraction using non-invasive approaches (e.g., optogenetics)
100 and limit decay in force generation for an extended period. We used Cre recombinase to induce
101 targeted expression of ChR2(H134R)-EYFP in Acta1-Cre mice and an optimized experimental
102 setup for *in vivo* muscle illumination in order to sustain contraction at the supraphysiological
103 activation duration of 1 second, and we showed the feasibility and repeatability of targeted
104 activation of the skeletal muscle *in vivo*.

105 **Methods**

106 *Animal model*

107 All procedures were approved by the Institutional Animal Care and Use Committee at the
108 University of Delaware (N = 21 mice). Mice were housed in same-sex cages (maximum of five
109 per cage) with littermates in BSL1 containment and monitored daily with regular chow and water
110 *ad libitum* with a 12hr on/12hr off light cycle. We used *in-vivo* Cre-lox recombination for
111 targeted expression of channelrhodopsin-2/YFP (ChR2(H134R)-EYFP) fusion protein (Ai32) in
112 skeletal muscle.¹⁶ To generate these mice, we crossed doxycycline-inducible, skeletal muscle-
113 specific ACTA1-rtTA,tetO-cre male mice (Acta1-Cre; C57BL6J background) with Ai32 reporter
114 female mice (C57BL6J background) (Figure 1A).^{17,18} Doxycycline chow (Envigo) was provided
115 *ad libitum* at time of mating to dams and continued until pups were weaned at 3-4 weeks of age.
116 Offspring were genotyped using PCR (Transnetyx, TN, USA). Acta1-Cre; Ai32 homozygous
117 mice (experimental) were used for blue light-induced stimulation and heterozygous or
118 homozygous Ai32 (Cre-negative) offspring were used as controls. To verify Acta1-Cre

119 specificity to skeletal muscle, we similarly crossed Ai14 (tdTomato) reporter mice with Acta1-
120 Cre mice to generate Acta1-Cre; Ai14 reporters (N = 2).

121 *ChR2 location and nerve infiltration*

122 To visualize localization of the ChR2(H134R)-EYFP protein in the skeletal muscle and
123 nerve, we dissected the quadriceps muscle and the main femoral branch of the sciatic nerve from
124 Acta1-Cre; Ai32 mice at euthanasia (N = 2). Harvested tissues were fixed in 4% PFA,
125 cryoprotected in sucrose, mounted in OCT freezing medium (Sakura, CA, USA), and sectioned
126 at 30 μ m thickness. Collected slides were then imaged with an Imager A2 microscope (Carl
127 Zeiss, Germany).

128 *Optogenetic stimulation setup*

129 We constructed a custom system with a LED (455 nm, 900 mW, M455L3, Thorlabs, NJ,
130 USA), a collimator (SM2F32-A; 350-700 nm, Thorlabs, NJ, USA) to reduce energy dissipation,
131 and high-power 1-Channel LED Driver (DC2200, Thorlabs, NJ, USA) for pulse modulation. The
132 LED driver interface was custom programmed to induce user-defined pulsatile light activation
133 intervals using LabView (National Instruments, TX, USA).

134 *Mouse preparation*

135 Mice were anesthetized using isoflurane administration (1-2%). Hair was removed from
136 hindlimb at the triceps surae muscle using chemical hair remover (Nair, Church & Dwight Co.,
137 NJ, USA). Animals were placed on a heating pad (Stoelting, IL, USA) at 37 °C in the prone
138 position and their hindlimb was placed in a modular *in-vivo* muscle stimulation apparatus
139 (Aurora Scientific, ON, Canada). The foot was placed in the footplate connected to a servomotor,
140 with the ankle axis of rotation aligned with and tibial axis perpendicular to the servomotor shaft.

141 The hindlimb was then clamped at the knee to stabilize the joint construct at 90° tibiofemoral
142 joint angle for isometric muscle contractions. Real-time measurements of applied ankle torque to
143 the foot pedal during light-induced plantar flexion were collected with a 1 N force transducer
144 (Aurora Scientific, ON, Canada).

145 *Muscle testing paradigm*

146 We used an iterative process to determine suggested optogenetic stimulation parameters
147 to increase the light-induced generated peak isometric ankle torque and obtain sustained
148 submaximal contractions. Short-duration (twitch-like) light exposure was administered to
149 exposed skin. The ankle torque was measured and the distance between skin and LED and the
150 collimator lens displacement were selected at the corresponding values to higher measured
151 isometric ankle torque readouts. Subsequently, the stimulation protocol (on and off) was adjusted
152 to increase peak isometric ankle torque readout. To determine the frequency for sustained muscle
153 contraction and minimize decay in contraction profile, we evaluated peak isometric torque at
154 each stimulation frequency and ankle torque profiles in male Acta1-Cre; Ai32 mice (N = 3;
155 Male; 3 months of age). The triceps surae muscles were stimulated at two different frequencies
156 of 10 Hz (70 ms on-/30 ms off-time; 10 repetitions; 1 second total duration) and 40 Hz (20 ms
157 on-/5 ms off-time; 40 repetitions; 1 second total duration). We selected 10 Hz stimulation as the
158 optimized stimulation protocol for sustaining muscle contraction and used this protocol for the
159 remainder of this study.

160 *Optimization and repeatability experiments*

161 Variations in optogenetic stimulation are dependent on: (1) strength of stimulus (power of
162 LED), (2) duration of stimulus (frequency used in protocol), and (3) cell type¹⁷. Therefore, we
163 evaluated the efficiency of our optogenetic setup by (1) measuring penetration of light (power

164 intensity) through the skin with the 10 Hz stimulation protocol; (2) measuring weight-dependent
165 generation of ankle torque, (3) assessing repeatability using contralateral limb experiments, and
166 (4) assessing contractile function of 10 Hz optogenetic stimulation compared to a comparable
167 duration of electrical stimulation.

168 *Power meter experiments*

169 We quantified the transmission of emission light intensity with a thermopile powermeter
170 sensor (Coherent PM10; 19 mm), with an appropriate wavelength sensitivity to the LED of use
171 (power 1150-1145 mW) to a and power meter (Fieldmate, Coherent). When placed at the
172 experimental fixed distance from the light source (Figure 2B), the percentage of light intensity
173 loss through the skin was determined through fresh dissected hairless skin patches from the
174 abdomen and back of euthanized mice. In each case, power readouts divided by active sensor
175 area (19 mm) to calculate light intensity.

176 *Weight-dependent response of optogenetic activation*

177 The weight-dependence of optogenetic stimulation *in vivo* was assessed in Triceps surae
178 muscle of Acta1-Cre; Ai32 male mice at 1.5, 3, 4, and 6-months of age (N = 2/age). Optical
179 stimulation was at 10 Hz protocol as previously described with ankle torque recorded.

180 *Electrical vs. optogenetic activation*

181 The right hindlimb of adult Acta1-Cre; Ai32 mice (N = 4; 2 males and 2 females, >3-
182 months of age) was randomly assigned to either optogenetic or electrical activation of the
183 Triceps surae with the contralateral limb assigned to the other. Optogenetic stimulation was a 10
184 Hz stimulation protocol (70 ms on time, 30 ms off time, 5 reps), electrical stimulation was with a
185 tetanic pulse trains (0.3 (ms) pulse width, 150 (Hz) pulse frequency, 0.5 (s) duration) via sub-
186 dermal PTFE-coated stainless steel EMG needle electrodes placed at the posterior knee and

187 distal Achilles to activate the tibial nerve. We chose not to sever peroneal nerve for inhibition of
188 antagonist anterior crural muscles contraction to maintain a non-invasive stimulation protocol
189 comparable the stimulation using optogenetics. Stimulations were repeated for three consecutive
190 days with ankle torque as the end-point measure. Measured torque values (mN.m) were
191 normalized to body mass (kg) to account for mouse weight variability.

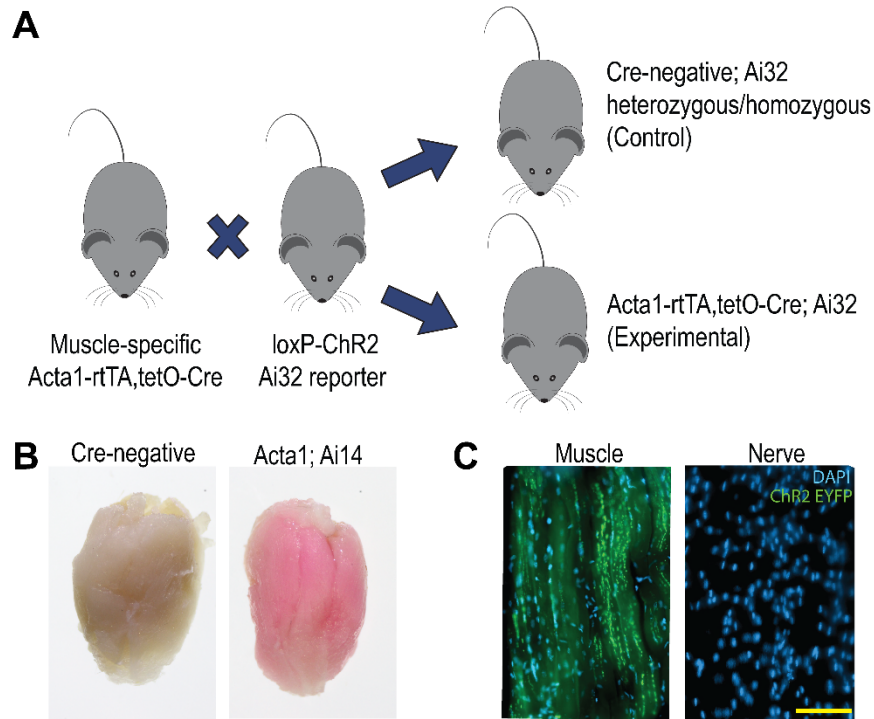
192 *Statistical analysis*

193 Peak measured ankle torque values from electrical and optogenetic stimulation were
194 statistically analyzed using two-way ANOVA with repeated measures or paired t-tests. The
195 relationship between bodyweight and peak measured ankle torque was determined by linear
196 regression. All statistical analyses were performed in Prism (version 7, Graphpad, LaJolla, CA).

197 **Results**

198 *Confirmation of Acta1-Cre specificity and expression of Ai32 in muscle*

199 Acta1-Cre Ai14 mice expressed robust tdTomato fluorescence in skeletal muscle
200 following cre recombination, verifying the lineage tracing of Acta1-Cre (Figure 1B). Results
201 from fluorescence imaging of nerve and skeletal muscle also showed that while ChR2(H134R)-
202 EYFP was strongly expressed in skeletal muscle, it had no specific expression in the main
203 femoral sciatic nerve branch (Figure 1C).



204

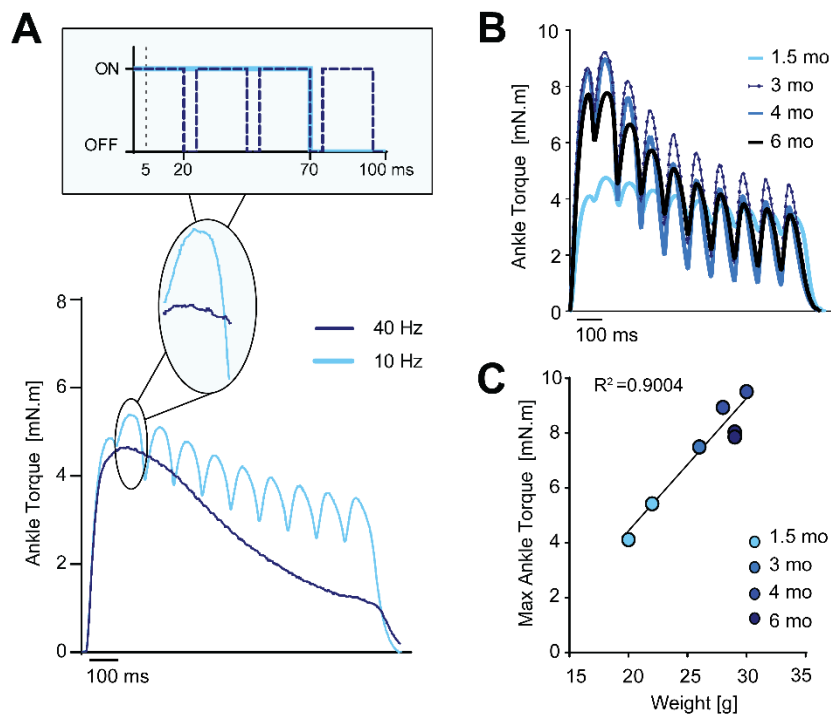
205 **Figure 1:** (A) Schematic showing the breeding scheme used for generation of experimental
206 (Acta1-Cre Ai32) and control (Cre-negative) mice. (B) Whole-mount triceps surae muscle (TS)
207 of Control and Acta1-Cre; tdTomato mice. (C) ChR2 was expressed in the skeletal muscle fibers
208 but was not expressed in the sciatic nerve using the Acta1-promoter. Scale bar denotes 100 μ m.

209 *Optimization*

210 We were able to induce muscle contraction using transdermal exposure to blue light with
211 Light On-Off optimization experiments (Supplemental Figure 2A, B) revealing 70 ms-On:30 ms
212 -Off as optimal. Furthermore, we show that 10 Hz light stimulation for 1000 ms elicited a
213 partially fused yet sustained tetanic plateau with higher frequency (40 Hz) exhibiting tetanic
214 plateau decay (Figure 2A). Despite variable plateau decay, peak force was stable during repeated
215 optogenetic stimulation (Supplemental Figure 3C). Despite a 74-80% reduction of light intensity

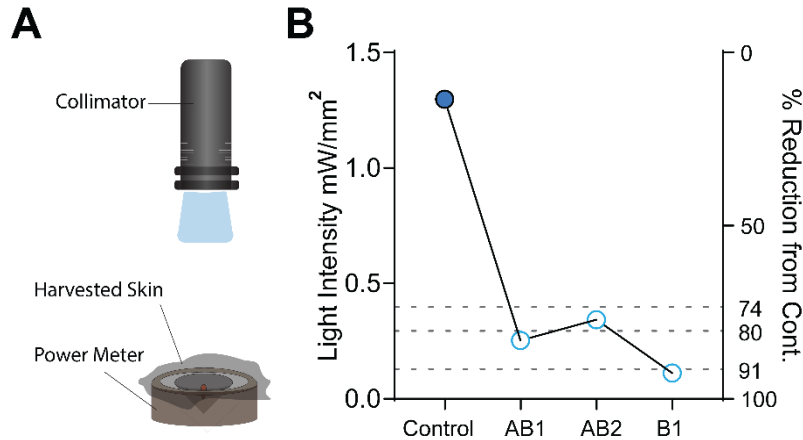
216 through abdominal skin and 91% reduction through back skin, we showed that the light intensity
217 was maintained at 0.26 and 0.35 mW/mm² respectively (Figure 3).

218 The magnitude of generated ankle torque under blue light stimulation correlated with the
219 weight of the mice, as expected (Figure 2B and C, $R^2 = 0.9004$, $p < 0.001$). Our method also
220 generated repeatable muscle contractions in contralateral limbs (Supplemental Figure 3A, B) and
221 in young adult mice of differing ages.



222

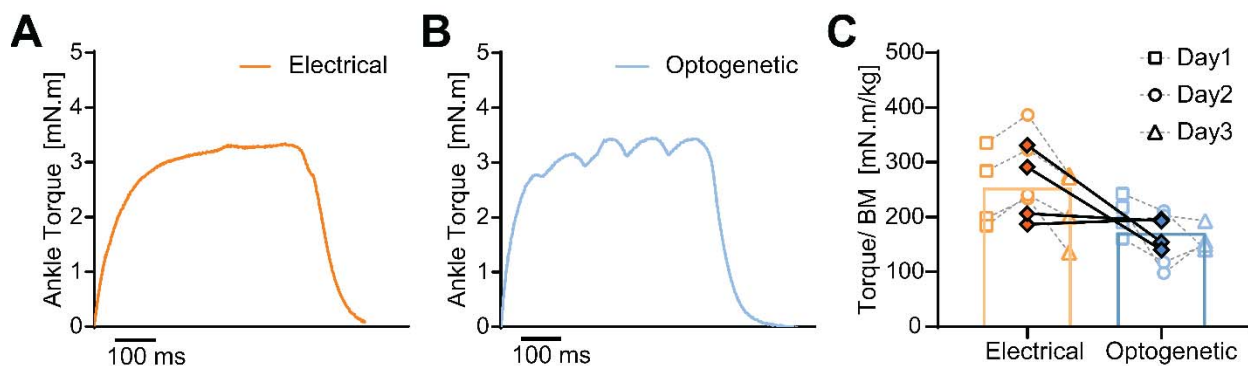
223 **Figure 2:** (A) Representative ankle torque profiles during 1 sec duration stimulation, comparing
224 10 Hz and 40 Hz. (B) Representative profile of generated ankle torque using 70 ms on/30 ms off
225 blue light stimulation for different aged mice. (C) Light-activated ankle torque was linearly
226 correlated with mouse weight ($R^2=0.9004$).



227

228 **Figure 3.** (A) Schematic of the experimental setup for light intensity measurements through
229 collected skin. (B) Although the transdermal delivery of blue light reduced the light intensity, it
230 still maintains an intensity of 0.2-0.3mW/mm². AB = abdominal skin; B = back skin.

231 Finally, in comparison to electrical stimulation of tibial nerve (Figure 4A), our optimized
232 pulsed optogenetic stimulation of 10 Hz (Figure 4B) resulted in comparable ankle torque values
233 (Figure 4C) and measurements are repeatable for each stimulation protocol across three
234 consecutive days.



235

236 **Figure 4.** (A) Representative ankle torque profiles for electrical stimulation (0.3 ms pulse
237 duration; 150Hz frequency; 0.5 sec duration) and (B) optogenetic stimulation (0.5 sec duration;

238 10Hz). (C) The average peak ankle torque generated during stimulations was comparable or
239 slightly reduced for optogenetics stimulation compared to electrical stimulation.

240 **Discussion**

241 Our findings demonstrate the feasibility and repeatability of optogenetics for non-invasive
242 plasmalemmal stimulation of skeletal muscle using *in vivo*. Using cre-lox recombinase system,
243 we induce targeted expression of channelrhodopsin-2/YFP in skeletal muscle (Acta1-Cre). We
244 showed that targeted expression of ChR2 in Acta1-Cre enables nerve-independent activation of
245 skeletal muscle *in vivo* and has comparable contractile function to that induced by electrical
246 stimulation of tibial nerve in native muscle construct.

247 We confirmed the feasibility of muscle contraction via direct light exposure through the
248 skin, despite light intensity reduction, and measured the light intensity. Light transmission
249 through hairless abdominal and back skin maintained an intensity of 0.2-0.3mW/mm² that is in
250 agreement with the previously reported minimum light intensity of 0.35 mW/mm² in skeletal
251 muscle stimulation for soleus muscle explants without first passing light through skin.¹¹ In this
252 study, we showed that our experimental setup exceeds the minimum delivery of light intensity
253 from our blue LED light source even after passing through skin from the trunk, which is more
254 thick than skin from the limbs.

255 The goal of our experiments was to develop a method for sustaining muscle contraction
256 using non-invasive approaches (e.g., optogenetics) and limit decay in force generation for an
257 extended period of time. We successfully optimized our experimental setup by controlling the
258 light intensity and pulse duration because we found that continuous illumination of light resulted
259 an unsustainable contraction force profile. As we increased pulse duration, we found that the

260 maximum force generation increased until we reached 70ms duration, which matched
261 previously-reported findings by Bruegmann et al.¹¹ In this same study, Bruegmann et al. also
262 linked the repetition rate of light stimulation to effective depolarization and repolarization of
263 membrane potentials in order to generate sustained muscle contraction, where repetition rates
264 >40 Hz reduced the efficiency of optogenetic stimulation.¹¹ The duty cycle of on/off time for
265 optogenetic stimulation is a critical factor for generating muscle contraction. Here, we showed
266 that the duration of light exposure generated the largest relative ankle torque at ~70ms, and this
267 finding was similar to previously reported durations of >70ms for ChR2 receptors to induce
268 depolarization more efficiently (at lower threshold) compared to electrical stimulation in
269 cardiomyocytes.¹⁹ The off-duty cycle is also important, as it allows the membrane to repolarize.
270 In this study, we found the decay profile to be sustained at higher forces when using a longer (
271 30ms) off-time between individual light pulses compared to shorter (10ms) off-time. This
272 finding aligned with work by others that reported a deactivation time constant for ChR2 at ~20
273 ms in order to obtain sufficient repolarization of lipid membrane between activations.¹² The
274 combination of both on- and off-duty cycling times are likely synergistic, and our comparisons
275 of 10Hz and 40Hz repetition rates underscores the importance of repolarization for maintaining
276 sustained contraction. Based on results from our study and two previous studies of optogenetic
277 activation in intact mammalian skeletal muscle, we suggest that an effective illumination
278 protocol (including both light intensity and pulsatile stimulation parameters) must be found
279 based on anatomical site, ChR2 expression method, and experimental approach in future
280 studies.^{11,12}

281 Finally, in this study, we showed that using an optimized optogenetic stimulation
282 protocol (10 Hz), we can induce increased and sustained muscle force generation, comparable to

283 that of electrical stimulation. It is noteworthy that the results from electrical stimulation of the
284 hindlimb in our study are lower in comparison to reported values in literature in stimulation of
285 plantar flexor muscle construct with peroneal nerve severed to inhibit contraction.²⁰ However,
286 this may be explained by antagonist muscle contraction because, in our study, we kept the
287 peroneal nerve intact during our hind limb stimulation. We made this choice in order to keep the
288 *in vivo* muscle complex intact and comparable to optogenetic stimulation setup.

289 Challenges in maximal and repeatable direct optogenetic stimulation are linked to: (1)
290 restricted recruitment of muscle fibers due to light absorption of myoglobin¹¹ and (2) differences
291 in myotube maturation level and the response of myotubes to excitation.¹⁰ Responsive cell
292 distribution and ChR2 expression level are fundamental for efficiency of opsin excitation, as
293 overexpression of ChR2 and its variants are needed to overcome low conductance and
294 desensitization of the opsin. Yet high opsin expression can be disruptive to the basal lipid
295 membrane voltage.²¹ Hence, a potential limitation of Cre-dependent expression of ChR2 is that
296 we may not be able to tune and distribute expression of ChR2. However, in this study, we used a
297 doxycycline-inducible and skeletal muscle-specific Cre which improved the specificity and can
298 allow for temporal control of ChR2 expression for future studies.

299 Future studies should focus on whether ChR2 stimulation in skeletal muscle increases the
300 leak currents within neighboring cell bodies (i.e. resting membrane potential, membrane
301 resistance, and action potential in surrounding skeletal muscle cell-not exposed to light- changes
302 compared to non-excited controls). This model is easily adjustable and, therefore, the stimulation
303 protocol can be further optimized to reduce inter-pulse relaxations and improve the contractile
304 profile under optical stimulation. In this study we showed the feasibility of optogenetic
305 stimulation in Acta1-Cre Ai32 mice and to sustain muscle contraction for extended

306 supraphysiological levels. It has been suggested that light stimulation might be more energy
307 efficient in contraction of cardiomyocytes compared to electrical stimulation.⁷ At short pulses,
308 AP morphology is similar between electrical and optogenetic stimulation; longer stimulation
309 durations, however, result in apparent longer plateau phase that may be in part caused by the
310 intrinsic negative feedback control of ChR2 activation.¹⁹ In future, effects of sustained prolonged
311 contraction on excitation contraction coupling during light stimulation compared to electrical
312 stimulation should be characterized. Lastly, measurement of *in vivo* electrophysiology in the
313 light-sensitive cells under blue light using patch clamp analysis, and quantification of the delay
314 in excitation in *in vivo* optogenetic stimulation compared to electrical stimulation would be
315 informative in characterization of our proposed model.

316 Direct optogenetic stimulation shows promising application for restoration of function and
317 atrophy caused by muscle denervation. Optogenetic muscle activation has recently been explored
318 skeletal and facial muscle complexes.^{11,12,22-24} In mice, studies have shown direct optogenetic
319 stimulation to improve functional metrics in denervated mouse whisker pads.²³ Others have used
320 Sim1-Ai32 transgenic mouse line, with non-specific expression in skeletal muscle t-tubule and
321 sarcolemma, to attenuate denervation-caused skeletal muscle atrophy using repeated optogenetic
322 stimulation.¹² In addition to transgenic mouse models, transplantation of murine embryonic
323 stem-cell derived motor neurons for targeted light stimulation of ChR2 in denervated sciatic
324 nerve branch improved function of denervated muscle.²⁴ However, applicability of optogenetic
325 stimulation can be expanded to study load-dependent development and maturation of
326 musculoskeletal tissues in juvenile mice. Muscle loading is critical for the healthy development
327 of musculoskeletal tissues.²⁵⁻²⁷ In in case of entheses, others have shown that unloading of this
328 tissue using intermuscular injection of botulinum toxin A in supraspinatus muscle is disruptive to

329 the development of functionally graded supraspinatus enthesis.²⁸ Role of increased muscle
330 loading on structure and function of the developing enthesis, however, is not well understood in
331 the field due technical limitations related to stimulating the growing muscle in neonatal mice
332 using standard approaches such as electrical stimulation and treadmill training. Direct
333 optogenetic stimulation can be widely utilized as a tool for non-invasive tools induce muscle
334 contraction for better understanding the mechanobiological cascades involved in formation and
335 homeostasis of the enthesis *in vivo*.

336 **Conclusion**

337 *In vivo* and direct optogenetic stimulation of skeletal muscle is a promising tool that can
338 also be used in conjunction with denervation models to study muscle regeneration. Optogenetics
339 can be used as a non-invasive toolbox for investigating the complex mechanobiological cascades
340 involved in development of skeletal tissues and effect of muscle loading on adjacent tissue (e.g.,
341 tendon) formation and adaptation. Our model has the potential to overcome the systemic
342 challenges and limitations of the existing models for muscle loading in the study of development
343 of tendon, enthesis, and bone.

344 References

- 345 1. Boyden ES, Zhang F, Bamberg E, Nagel G, Deisseroth K. Millisecond-timescale,
346 genetically targeted optical control of neural activity. *Nat Neurosci.* 2005;8(9):1263-1268.
347 doi:10.1038/nn1525
- 348 2. Boyden ES. A history of optogenetics: The development of tools for controlling brain
349 circuits with light. *F1000 Biol Rep.* 2011;3(1). doi:10.3410/B3-11
- 350 3. Nagel G, Szellas T, Huhn W, et al. Channelrhodopsin-2, a directly light-gated cation-
351 selective membrane channel. *Proc Natl Acad Sci.* 2003;100(24):13940-13945.
352 doi:10.1073/pnas.1936192100
- 353 4. Deisseroth K. Optogenetics. *Nat Methods.* 2011;8(1):26-29. doi:10.1038/nmeth.f.324
- 354 5. Parr-Brownlie LC, Bosch-Bouju C, Schoderboeck L, Sizemore RJ, Abraham WC, Hughes
355 SM. Lentiviral vectors as tools to understand central nervous system biology in
356 mammalian model organisms. *Front Mol Neurosci.* 2015;8(MAY):1-12.
357 doi:10.3389/fnmol.2015.00014
- 358 6. Boyle PM, Williams JC, Ambrosi CM, Entcheva E, Trayanova NA. A comprehensive
359 multiscale framework for simulating optogenetics in the heart. *Nat Commun.* 2013;4(1):1-
360 9. doi:10.1038/ncomms3370
- 361 7. Jia Z, Valiunas V, Lu Z, et al. Stimulating cardiac muscle by light cardiac optogenetics by
362 cell delivery. *Circ Arrhythmia Electrophysiol.* 2011;4(5):753-760.
363 doi:10.1161/CIRCEP.111.964247
- 364 8. Bruegmann T, Malan D, Hesse M, et al. Optogenetic control of heart muscle in vitro and

- 365 in vivo. *Nat Methods*. 2010;7(11):897-900. doi:10.1038/nmeth.1512
- 366 9. Alexander Quinn T, Schneider-Warme F, Sasse P, L-H Huang C, Ferenczi EA, Tan X.
367 Optogenetic Methods in Cardiac Systems *Frontiers in Physiology* | www. *Front Physiol* /
368 *www.frontiersin.org*. 2019;1(2):1096. doi:10.3389/fphys.2019.01096
- 369 10. Asano T, Ishizua T, Yawo H. Optically controlled contraction of photosensitive skeletal
370 muscle cells. *Biotechnol Bioeng*. 2012;109(1):199-204. doi:10.1002/bit.23285
- 371 11. Bruegmann T, van Bremen T, Vogt CC, Send T, Fleischmann BK, Sasse P. Optogenetic
372 control of contractile function in skeletal muscle. *Nat Commun*. 2015;6(1):7153.
373 doi:10.1038/ncomms8153
- 374 12. Magown P, Shettar B, Zhang Y, Rafuse VF. Direct optical activation of skeletal muscle
375 fibres efficiently controls muscle contraction and attenuates denervation atrophy. *Nat*
376 *Commun*. 2015;6(1):1-9. doi:10.1038/ncomms9506
- 377 13. Ishizuka T, Kakuda M, Araki R, Yawo H. Kinetic evaluation of photosensitivity in
378 genetically engineered neurons expressing green algae light-gated channels. *Neurosci Res*.
379 2006;54(2):85-94. doi:10.1016/j.neures.2005.10.009
- 380 14. Brecht M, Schneider M, Sakmann B, Margrie TW. Whisker movements evoked by
381 stimulation of single pyramidal cells in rat motor cortex. *Nature*. 2004;427(6976):704-
382 710. doi:10.1038/nature02266
- 383 15. Towne C, Montgomery KL, Iyer SM, Deisseroth K, Delp SL. Optogenetic Control of
384 Targeted Peripheral Axons in Freely Moving Animals. *PLoS One*. 2013;8(8):72691.
385 doi:10.1371/journal.pone.0072691

- 386 16. Madisen L, Mao T, Koch H, et al. A toolbox of Cre-dependent optogenetic transgenic
387 mice for light-induced activation and silencing. *Nat Neurosci.* 2012;15(5):793-802.
388 doi:10.1038/nn.3078
- 389 17. Tanaka KF. Optogenetics research using the mouse as a model system. In: *Optogenetics:
390 Light-Sensing Proteins and Their Applications.* Springer Japan; 2015:227-240.
391 doi:10.1007/978-4-431-55516-2_15
- 392 18. Rao P, Monks DA. A tetracycline-inducible and skeletal muscle-specific Cre recombinase
393 transgenic mouse. *Dev Neurobiol.* 2009;69(6):401-406. doi:10.1002/dneu.20714
- 394 19. Williams JC, Entcheva E. Optogenetic versus electrical stimulation of human
395 cardiomyocytes: Modeling insights. *Biophys J.* 2015;108(8):1934-1945.
396 doi:10.1016/j.bpj.2015.03.032
- 397 20. Southern WM, Nichenko AS, Shill DD, et al. Skeletal muscle metabolic adaptations to
398 endurance exercise training are attainable in mice with simvastatin treatment. 2017.
399 doi:10.1371/journal.pone.0172551
- 400 21. Lin JY. A user's guide to channelrhodopsin variants: Features, limitations and future
401 developments. *Exp Physiol.* 2011;96(1):19-25. doi:10.1113/expphysiol.2009.051961
- 402 22. Park S, Bandi A, Lee CR, Margolis DJ. Peripheral optogenetic stimulation induces
403 whisker movement and sensory perception in head-fixed mice. *Elife.* 2016;5(JUNE2016).
404 doi:10.7554/eLife.14140
- 405 23. Vajtay TJ, Bandi A, Upadhyay A, et al. Optogenetic and transcriptomic interrogation of
406 enhanced muscle function in the paralyzed mouse whisker pad. *J Neurophysiol.*

- 407 2019;121(4):1491-1500. doi:10.1152/jn.00837.2018
- 408 24. Bryson JB, Machado CB, Crossley M, et al. Optical control of muscle function by
409 transplantation of stem cell-derived motor neurons in mice. *Science* (80-).
410 2014;344(6179):94-97. doi:10.1126/science.1248523
- 411 25. Frost HM. Wolff's Law and bone's structural adaptations to mechanical usage: an
412 overview for clinicians. *Angle Orthod.* 1994;64(3):175-188. doi:10.1043/0003-
413 3219(1994)064<0175:WLABSA>2.0.CO;2
- 414 26. Duncan RL, Turner CH. Mechanotransduction and the functional response of bone to
415 mechanical strain. *Calcif Tissue Int.* 1995;57(5):344-358. doi:10.1007/BF00302070
- 416 27. Killian ML, Cavinatto L, Galatz LM, Thomopoulos S. The role of mechanobiology in
417 tendon healing. *J Shoulder Elb Surg.* 2012;21(2):228-237. doi:10.1016/j.jse.2011.11.002
- 418 28. Schwartz AG, Lipner JH, Pasteris JD, Genin GM, Thomopoulos S. Muscle loading is
419 necessary for the formation of a functional tendon enthesis. *Bone.* 2013;55(1):44-51.
420 doi:10.1016/j.bone.2013.03.010
- 421